Monatsh Chem (2009) 140:1–8
DOI 10.1007/s00706-008-0018-1

ORIGINAL PAPER

The effect of sodium benzoate and sodium 4-(phenylamino)benzenesulfonate on the corrosion behavior of low carbon steel

Badiea A. Mohammed · Kikkeri N. Mohana

Received: 20 February 2008 / Accepted: 2 June 2008 / Published online: 22 August 2008

Abstract The effect of sodium benzoate (SB) and sodium 4-(phenylamino)benzenesulfonate (SPABS) on the corrosion behavior of low carbon steel has been investigated using gravimetric method in the temperature range of 30–80 °C, velocity range of 1.44–2.02 m s^{-1} and concentration range of 6.94×10^{-4} to 4.16×10^{-3} mol dm^{-3} SB and 3.69×10^{-4} to 2.06×10^{-3} mol dm^{-3} SPABS. Optimization of temperature, fluid velocity, and inhibitors concentration has been made. The obtained results indicate that the inhibition efficiency (w_{IE} %) at 1.56 m s^{-1} is not in excess of 81.5% at 4.16×10^{-3} mol dm^{-3} SB and 84.4% at 2.06×10^{-3} mol dm^{-3} SPABS. The inhibitive performance of these compounds showed an improvement with increasing concentration up to critical values of SB and SPABS; beyond these concentrations no further effectiveness is observed. These inhibitors retard the anodic dissolution of low carbon steel by protective layer bonding on the metal surface. The adsorption of SB and SPABS on the low carbon steel surface was found to obey the Freundlich isotherm model. The FT-IR spectroscopy was used to analyze the surface adsorbed film.

Keywords Fluid velocity · Industrial water · Low carbon steel · Sodium benzoate · Sodium 4-(phenylamino)benzenesulfonate

B. A. Mohammed · K. N. Mohana (✉)
Department of Studies in Chemistry,
University of Mysore, Manasagangotri,
Mysore 570006, India
e-mail: knmsvp@yahoo.com

Introduction

Addition of inhibitors is still one of the requirements to protect metals and alloys against attack in many industrial environments. Hence, the development of new inhibitors based on organic compounds containing nitrogen, oxygen and sulfur atoms is of growing interest in the field of chemical industries to solve corrosion problems and reduce the economic cost of equipment [1]. The efficiency of these inhibitors depends on chemical composition, structure of inhibitors, nature and state of the metallic surface, and the nature of the environment. Most organic inhibitors are adsorbed on the metal surface by displacing water molecules and forming a compact barrier film [2–4]. The molecules that contain both nitrogen and sulfur in their structure are of particular importance, since these provide an excellent inhibition compared with the compounds that contain only sulfur or nitrogen [5–8]. The selection of a suitable inhibitor mainly depends on the type of industrial environment, type of ions it contains, velocity of the fluid and environment temperature. Most of the efficient inhibitors used in industries are organic compounds having multiple bonds in their molecules containing nitrogen and sulfur atoms [9], and are adsorbed on the metal surface. Adsorption depends on the possible interaction of a π-orbital of the inhibitor with a *d*-orbital of the metal atoms, which induces greater adsorption of the inhibitor molecules on the carbon steel surface leading to the formation of a protective film on the metal surface.

Laminar and turbulent flow are two categories of water flow [10]. Laminar flow is low in velocity and may not be consistent across the metal surface. Turbulent flow is at a higher velocity and acts by reducing the laminar layer along the surfaces. Also, appropriate fluid velocity is necessary for proper distribution of inhibitors.

SB and SPABS are advised to be used as good protective inhibitors, particularly in low carbon steel pipes used for carrying oil and gas that contain a higher content of water. They are non-toxic, low cost, and friendly for the environment. SB and SPABS can be used in the protection of heat exchangers, reboiler tubes, and refinery units against aggressive normal and industrial water used for cooling or heating the equipment and products during the industrial processes. In the light of the available information, the present paper reports the results of our investigation on the inhibitive performance of SB and SPABS on low carbon steel, at various velocities and temperatures, of industrial water using the mass loss method. The adsorption thermodynamic parameters were evaluated and isotherm behavior has been determined.

Results and discussion

Adsorption isotherm

In order to understand the corrosion process on low carbon steel, adsorption characteristics were studied in the temperature range of 30–80 °C. The adsorption isotherm was drawn and the related mechanism was determined. The degree of the surface coverage (w_{IE}), is related to an adsorption constant (K_{ads}) which is related to Gibbs energy of adsorption according to Eqs. (3) and (4). In order to assign the performance of the inhibitor, inhibition efficiency (w_{IE} %) was calculated, and the relationships between the performance and other effective parameters were obtained. The surface coverage (w_{IE}) and inhibition efficiency (w_{IE} %) have been calculated from mass loss measurements using the following equations:

$$w_{IE} = 1 - \frac{(v_{cor})_p}{(v_{cor})_a}, \quad w_{IE}\,\% = \left(1 - \frac{(v_{cor})_p}{(v_{cor})_a}\right) \times 100 \qquad (1)$$

where $(v_{cor})_p$ and $(v_{cor})_a$ are the corrosion rate in the presence and absence of the inhibitor, as calculated by using Eq. (10). The values of v_{cor}, w_{IE} %, and w_{IE} are given in Table 1. The adsorption process between the organic molecules in the aqueous solution and the water molecules on the metallic surface is expressed as below [11]:

$$Org_{(sol)} + XH_2O_{(ads)} \rightleftharpoons Org_{(ads)} + XH_2O_{(sol)} \qquad (2)$$

where $Org_{(sol)}$ and $Org_{(ads)}$ are the organic molecules in the aqueous solution and that adsorbed on the metallic surface, respectively. $H_2O_{(ads)}$ represents the water molecules on the metallic surface, and X is the size ratio representing the number of water molecules replaced by one molecule of organic adsorbate. In the present investigation, the Freundlich isotherm was found to be the best description for the process. The isotherm is described by Eq. (3).

$$w_{IE} = (K_{ads} \cdot c)^n; \quad 0 < n < 1 \qquad (3)$$

where c is the inhibitor concentration (mol dm^{-3}) and K_{ads} is the adsorption equilibrium constant (dm^3 mol^{-1}). The correlation coefficient R^2 was used to determine the best isotherm which describes the adsorption process (Table 2). Using Eq. 3, plots of log w_{IE} versus log c, gave straight lines (Fig. 1a, b) with a slope more than zero and less than unity, confirming the applicability of the Freundlich isotherm. The adsorption equilibrium constant (K_{ads}) is related to the standard Gibbs energy of adsorption ($\Delta_{ads}G$) with the following Eq. (4):

$$K_{ads} = \frac{1}{55.5}\exp\left(-\frac{\Delta_{ads}G}{RT}\right). \qquad (4)$$

Here, 55.5 is the molar concentration of water in solution (mol dm^{-3}), R is the universal gas constant and T is the absolute temperature. The values of $\Delta_{ads}G$ and K_{ads} at various temperature are listed in Table 2. From Table 2, it is shown that $(\partial G/\partial t)_{T,P} < 0$, indicating that the Gibbs function was decreasing. Therefore, the adsorption processes of SB and SPABS on a low carbon steel surface in industrial water is spontaneous under the experimental conditions employed. Nageh Allam and Benali et al. [12, 13] reported that the values of $-\Delta_{ads}G$ of the order of 20 kJ mol^{-1} or lower indicate a physisorption and those of the order of 37 kJ mol^{-1} or higher show chemisorption. In the present study, the values of $-\Delta_{ads}G$ obtained varied from 21.65 to 25.71 kJ mol^{-1} for SB and from 24.40 to 28.51 kJ mol^{-1} for SPABS, indicating that the adsorption mechanism for both inhibitors on low carbon steel surface in industrial water is physisorption.

The enthalpy ($\Delta_{ads}H$) and entropy ($\Delta_{ads}S$) of adsorption on low carbon steel in industrial water in the presence of the inhibitors can be calculated by using the following equation:

$$\ln K_{ads} = \ln\left(\frac{1}{55.5}\right) - \frac{\Delta_{ads}H}{RT} + \frac{\Delta_{ads}S}{R} \qquad (5)$$

Using Eq. (5), the values of $\Delta_{ads}H$ and $\Delta_{ads}S$ were evaluated from the slope and intercept of the plot of ln K_{ads} versus 1/T (Fig. 2). The thermodynamic data of adsorption are depicted in Table 2. The values obtained confirm the endothermic behavior of the adsorption process of SB and SPABS on the low carbon steel surface in industrial water. The values of $\Delta_{ads}S$ obtained are large and positive for both inhibitors indicating that an increase in disordering takes places in going from reactants to the metal adsorbed species of the reaction complex [14]. Further, the adsorption enthalpy is small and positive in the case of SPABS and positive in the case of SB, and the adsorption entropy is

Table 1 Corrosion parameters of low carbon steel surface in industrial water in the absence and presence of SB and SPABS at different temperatures and at 1.44 m s^{-1}

Temperature/K	Concentration/mol dm^{-3}		SB			SPABS		
	SB	SPABS	v_{cor}/g m^{-2} day^{-1}	w_{IE} %/%	w_{IE}	v_{cor}/g m^{-2} day^{-1}	w_{IE} %/%	w_{IE}
303	Blank		7.97	–	–	7.97	–	–
	6.94×10^{-4}	3.69×10^{-4}	5.11	35.89	0.3588	5.00	37.26	0.3726
	1.39×10^{-3}	5.53×10^{-4}	4.02	49.55	0.4956	4.10	48.56	0.4856
	2.78×10^{-3}	9.22×10^{-4}	3.52	55.82	0.5582	3.45	56.71	0.5671
	3.47×10^{-3}	1.66×10^{-3}	2.45	69.31	0.6931	2.27	71.52	0.7152
	4.16×10^{-3}	2.06×10^{-3}	1.99	75.04	0.7504	1.46	81.68	0.8168
313	Blank		8.77	–	–	8.77	–	–
	6.94×10^{-4}	3.69×10^{-4}	5.43	38.05	0.3805	5.40	38.43	0.3843
	1.39×10^{-3}	5.53×10^{-4}	4.11	53.14	0.5314	4.13	52.91	0.5291
	2.78×10^{-3}	9.22×10^{-4}	3.55	59.52	0.5952	3.27	62.71	0.6271
	3.47×10^{-3}	1.66×10^{-3}	2.61	70.22	0.7022	2.42	72.41	0.7241
	4.16×10^{-3}	2.06×10^{-3}	1.89	78.48	0.7848	1.66	81.07	0.8107
328	Blank		10.35	–	–	10.35	–	–
	6.94×10^{-4}	3.69×10^{-4}	6.30	39.17	0.3917	6.23	39.81	0.3981
	1.39×10^{-3}	5.53×10^{-4}	4.73	54.34	0.5434	4.87	52.95	0.5295
	2.78×10^{-3}	9.22×10^{-4}	3.83	63.02	0.6302	4.03	61.06	0.6106
	3.47×10^{-3}	1.66×10^{-3}	2.47	76.18	0.7618	2.65	74.40	0.7440
	4.16×10^{-3}	2.06×10^{-3}	2.00	80.69	0.8069	1.86	82.03	0.8203
343	Blank		16.91	–	–	16.91	–	–
	6.94×10^{-4}	3.69×10^{-4}	10.22	39.55	0.3955	9.97	41.04	0.4104
	1.39×10^{-3}	5.53×10^{-4}	7.89	53.38	0.5338	7.87	53.46	0.5346
	2.78×10^{-3}	9.22×10^{-4}	6.72	60.26	0.6026	6.40	62.15	0.6215
	3.47×10^{-3}	1.66×10^{-3}	4.19	75.22	0.7522	4.39	74.04	0.7404
	4.16×10^{-3}	2.06×10^{-3}	3.15	81.38	0.8138	2.64	84.31	0.8431
353	Blank		14.51	–	–	14.51	–	–
	6.94×10^{-4}	3.69×10^{-4}	8.79	39.40	0.3940	8.44	41.83	0.4183
	1.39×10^{-3}	5.53×10^{-4}	6.16	57.52	0.5752	6.89	52.52	0.5252
	2.78×10^{-3}	9.22×10^{-4}	5.09	64.93	0.6493	5.52	61.96	0.6196
	3.47×10^{-3}	1.66×10^{-3}	3.88	73.28	0.7328	3.82	73.67	0.7367
	4.16×10^{-3}	2.06×10^{-3}	2.89	80.12	0.8012	2.58	82.22	0.8222

Table 2 Thermodynamic parameters for adsorptions of SB and SPABS on low carbon steel in industrial water at different temperatures and at 1.44 m s^{-1}

Inhibitors	Temperature/K	K_{ads}/ dm^3 mol^{-1}	R^2	$\Delta_{ads}G$/ kJ mol^{-1}	$\Delta_{ads}H$/ kJ mol^{-1}	$\Delta_{ads}S$/ J mol^{-1} K^{-1}
SB	303	97.0	0.961	−21.65		
	313	125.5	0.982	−23.03		
	328	132.3	0.975	−24.28	2.65	81.30
	343	136.2	0.963	−25.47		
	353	114.9	0.966	−25.71		
SPABS	303	290.0	0.987	−24.40		
	313	292.8	0.971	−25.23		
	328	296.4	0.974	−26.48	0.47	82.11
	343	297.5	0.975	−27.70		
	353	297.6	0.986	−28.51		

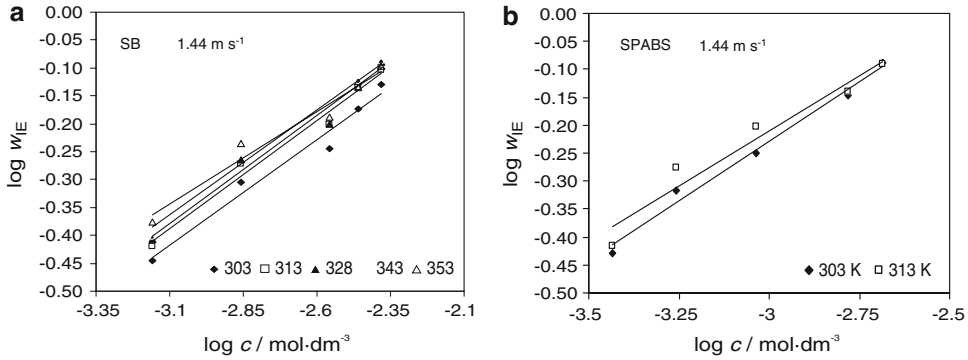

Fig. 1 Freundlich adsorption isotherm for SB (**a**) and SPABS (**b**) on the low carbon steel surface in industrial water media at 1.44 m s^{-1}

large and has positive values in both SB and SPABS, indicating that the driving force for the adsorption of adsorbate is the increase in the entropy during the processes of adsorption rather than the decrease in enthalpy [14]. The values of thermodynamic parameters for the adsorption of the inhibitors can provide valuable information about the mechanism of the corrosion inhibition. While an endothermic adsorption process ($\Delta_{ads}H > 0$) is attributed unequivocally to chemisorption [15], an exothermic adsorption process ($\Delta_{ads}H < 0$) may involve either physisorption or chemisorption or a mixture of both processes. But in the present study, the process of adsorption is physisorption because $-\Delta_{ads}G$ is lower than 37 kJ mol^{-1} and also the numerical values of n ($0 < n < 1$) are obviously less than 0.4 in both adsorption isotherms of SB and SPABS. Further, unfavorable isotherms occurred because relatively low solid loadings are obtained, which leads to quite long mass-transfer zones in the bed.

Effect of temperature

The influence of temperature on v_{cor} was studied in the presence and absence of the inhibitors at various concentrations of SB and SPABS and at various fluid velocities during 7 h of immersion. The v_{cor} of low carbon steel in industrial water in the absence of SB and SPABS increased with increasing temperature between 30 and 55 °C (Fig. 3). However, a remarkable increase was observed between 55 and 70 °C, and then it began decreasing at 80 °C. Furthermore, in the presence of inhibitors. the v_{cor} slightly changed with increasing temperature. The decrease in v_{cor} at 80 °C may be attributed to the escape of oxygen from the open system. Also, at higher temperatures, desorption occurs because the process obeys the Freundlich isotherm model (slope < 1). The Freundlich adsorption isotherm requires only a slightly higher temperature for desorption to occur whereas the Langmuir adsorption isotherm (slope = 1) requires a much higher temperature to begin desorption [16]. Moreover, the physisorption is completely reversible since the molecules are not tightly retained by the adsorbent [17]. From Fig. 4, it is evident that the w_{IE} % of SB increases with increasing temperature at optimum concentration and at 1.44 m s^{-1}, whereas in the case of SPABS, w_{IE} % is independent of temperature. Ivanov [18] reported the increase of w_{IE} % with temperature as the change in the nature of the

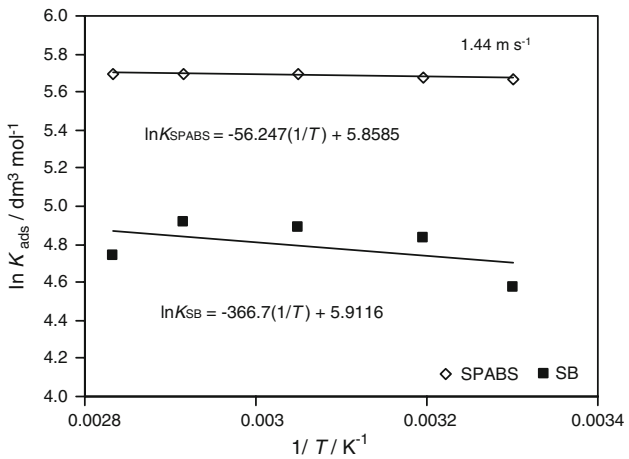

Fig. 2 Plots of ln K_{ads} against $1/T$ for SB and SPABS on low carbon steel in industrial water at 1.44 m s^{-1}

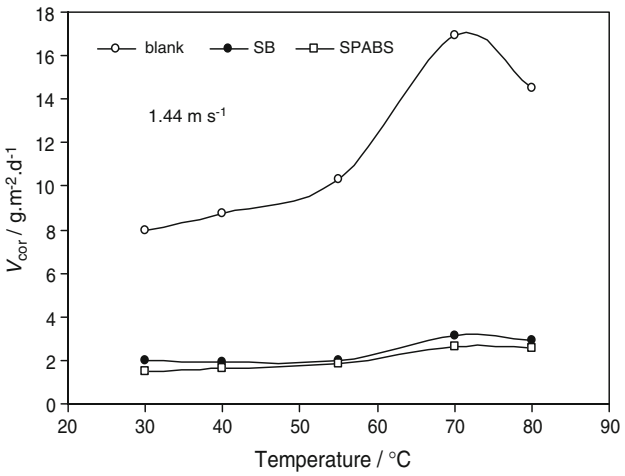

Fig. 3 Effect of temperature on v_{cor} of low carbon steel in industrial water at optimum concentrations of SB and SPABS and at 1.44 m s^{-1}

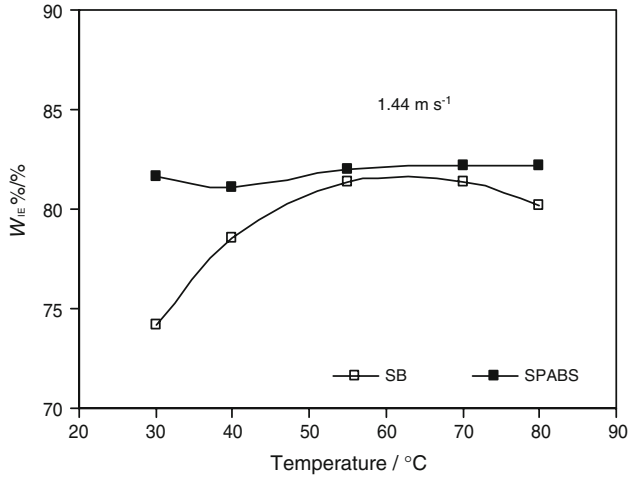

Fig. 4 Effect of temperature on the w_{IE} % of SB and SPABS on low carbon steel surface at optimum concentrations and at 1.44 m s^{-1}

adsorption mode. In the present investigation, SB undergoes chemisorption at lower temperature and at optimum concentration, but physisorption is favored as the temperature is increased. However, in the case of SPABS, the adsorption is physisorption at all temperatures (Fig. 4).

The activation energy (E_a) for the corrosion processes can be calculated from the Arrhenius equation:

$$v_{cor} = A \cdot \exp(-E_a/RT) \quad (6)$$

where E_a is the apparent activation energy, A is the Arrhenius pre-exponential constant. Plots of log (v_{cor}) versus 1/T in the absence and presence of inhibitors are shown in Fig. 5a, b. The values of E_a and A of the corrosion process for low carbon steel in industrial water were evaluated from the slopes and intercepts of the above plots. The values of E_a obtained with and without inhibitors are low indicating a slow corrosion rate of low carbon steel in industrial water. In addition, as w_{IE} % increases the E_a decreases, i.e., the highest performance of inhibitors is produced at the lowest value of activation energy for the corrosion process. From Table 3, it is clear that the higher rate is associated with higher activation energy and vice versa. This may be attributed to the change in the mechanism of the corrosion process in the presence of adsorbed inhibitor molecules [19]. Typically, from Eq. (6), the higher E_a and lower A lead to a decrease in the v_{cor}, but in the present work, the decrease in A with increasing concentrations of SB and SPABS leads to a decrease in v_{cor} of the low carbon steel surface in industrial water. Riggs and Hurd [20] reported that the decrease in E_a of corrosion rate at higher levels of inhibitor arises from a shift of the net corrosion reaction from the uncovered part on the metal surface to the covered one. Schmid and Huang [21] found that organic molecules inhibit both anodic and cathodic partial reactions on the electrode surface and that a parallel reaction takes place on the covered area.

The enthalpy and entropy of activation (ΔH_a and ΔS_a) can be computed by using the Eyring equation:

$$v_{cor} = \frac{RT}{Nh}\exp\left(\frac{\Delta S_a}{R}\right) \cdot \exp\left(\frac{-\Delta H_a}{RT}\right) \quad (7)$$

where N is Avogadro's constant and h is Plank's constant. Using the values of ln (v_{cor}/T) and $1/T$, ΔH_a and ΔS_a could be calculated from the slopes and intercepts at various concentrations of the studied inhibitors (Table 3).

The positive values of activation enthalpy reflect the endothermic behavior of low carbon steel dissolution processes in the presence and absence of both inhibitors. Large and negative values of activation entropy imply that the activated complex in the rate determining step represents an association rather than a dissociation step, which means a decrease in disordering takes place on going from reactants to the activated complex [22].

Effect of time

The effects of immersion time on mass loss per unit area of low carbon steel in uninhibited and inhibited industrial water at 55 °C and at 1.44 m s^{-1} were studied. It is obvious that the mass loss varied linearly with immersion

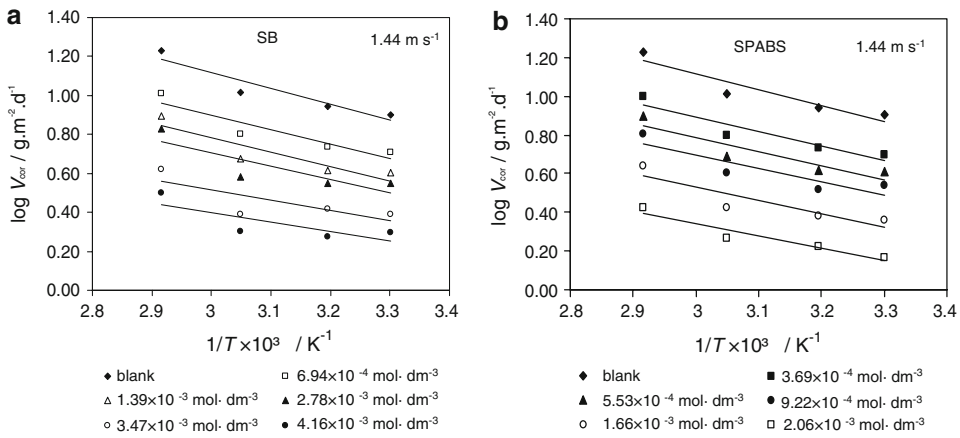

Fig. 5 Arrhenius plots of corrosion of low carbon steel in industrial water at different concentrations of SB (**a**) and SPABS (**b**) and at 1.44 m s^{-1}

Table 3 Values of activation parameters and pre-exponential factor (A) for low carbon steel in industrial water in the absence and presence of SB and SPABS at 1.44 m s^{-1}

Inhibitors	Concentration/ mol dm^{-3}	A/g m^{-2} day^{-1}	E_a/kJ mol^{-1}	ΔH_a/kJ mol^{-1}	ΔS_a/J mol^{-1} K^{-1}
SB	Blank	3,655.95	15.62	12.94	−185.69
	6.94×10^{-4}	1,436.48	14.41	11.73	−193.46
	1.39×10^{-3}	956.31	14.03	11.35	−196.84
	2.78×10^{-3}	572.14	13.10	10.42	−201.12
	3.47×10^{-3}	122.94	10.05	7.37	−210.56
	4.16×10^{-3}	121.53	8.62	6.77	−210.85
SPABS	3.69×10^{-4}	1,350.21	14.29	11.61	−193.98
	5.53×10^{-4}	884.50	13.79	11.01	−197.80
	9.22×10^{-4}	644.61	13.48	10.95	−199.62
	1.66×10^{-3}	418.89	13.34	10.85	−203.05
	2.06×10^{-3}	176.64	12.16	9.78	−209.94

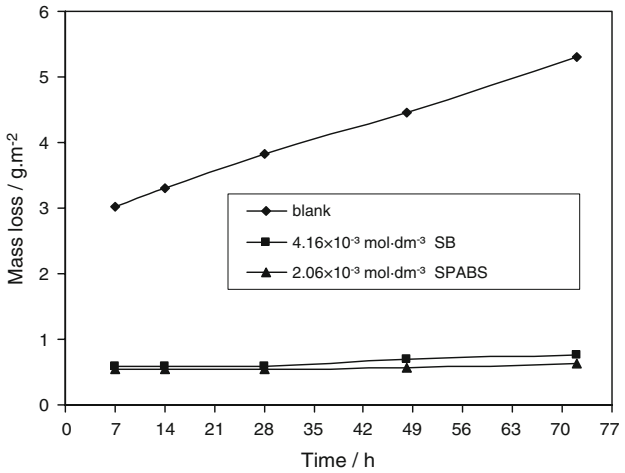

Fig. 6 Mass loss per unit area as a function of time for the low carbon steel corrosion in industrial water of added 4.16×10^{-3} mol dm^{-3} SB and 2.06×10^{-3} mol dm^{-3} SPABS at 55 °C and 1.44 m s^{-1}

period for both inhibitors and uninhibited solution (Fig. 6). In the absence of the inhibitors, the v_{cor} was clearly increasing linearly with increasing time (i.e., $dv_{cor}(t)/dt \neq 0$). The lines obtained in the presence of the inhibitors fall significantly below that of the free solution. It is evident that the mass loss per unit area in the presence of the inhibitors was nearly independent of immersion time ($dv_{cor}(t)/dt \approx 0$). The linear variation of mass loss with time in plain and inhibited solutions shows the absence of insoluble product on the low carbon steel surface. The relatively large divergence of the plots indicates the increase of w_{IE} % with time.

Effect of fluid velocity

The experiment was carried out at various rotational speeds of the specimen in industrial water. As the fluid flows through the pipe, the rotational speed of the specimen is converted into flow rate of the fluid using the following empirical equations [16]:

$$q = 0.92nD_a^3\left(\frac{D_t}{D_a}\right) \tag{8}$$

$$A_p = \pi D_a W \tag{9}$$

where q is the total flow rate from the edges of impeller (m^3 s^{-1}), n is the number of rotations per s, D_a is the impeller diameter (m), D_t is the diameter of the solution vessel (m), A_p is the area of the cylinder swept by the tips of the impeller blades (m^2), and W is the width of blades (m). The velocity of the fluid can be obtained by dividing Eq. (8) by Eq. (9). Butler and Stroud [23] studied the corrosion rate of mild steel tubes with high purity water and observed that the rate increased with increasing speed of flow to a maximum value of about 3.3 ft/s (1.006 m s^{-1}). Sinnott [24] reported that a maximum velocity of 4 m s^{-1} is required to reduce fouling, and that the velocity of water is appropriate between 1.5 and 2.5 m s^{-1}. In the present work, the corrosion rate of low carbon steel in the absence and presence of SB and SPABS increased with increasing velocity of the fluid (Fig. 7). The maximum w_{IE} % was observed at 1.56 m s^{-1}, and the performance of SPABS are relatively more than that of SB. This is due to the fact that, at 1.56 m s^{-1}, distribution of inhibitors is appropriate and the diffusion of dissolved oxygen might also encounter more difficulty in reaching the metal surface because of the existence the laminar layer. The maximum performance of inhibitors was observed at 4.16×10^{-3} mol dm^{-3} and 2.06×10^{-3} mol dm^{-3} for SB and SPABS, at all velocities and temperatures. The w_{IE} % then began decreasing beyond 1.56 m s^{-1}, because of impingement attack which is caused by the turbulent flow of solution over the metal surface. This is attributed to the fact that, at higher velocity, the extraneous impurities such as sand, dust, and scales, etc., embedded on the metal surface causes pitting or scratching to the molecules of the absorbed layer and removes the

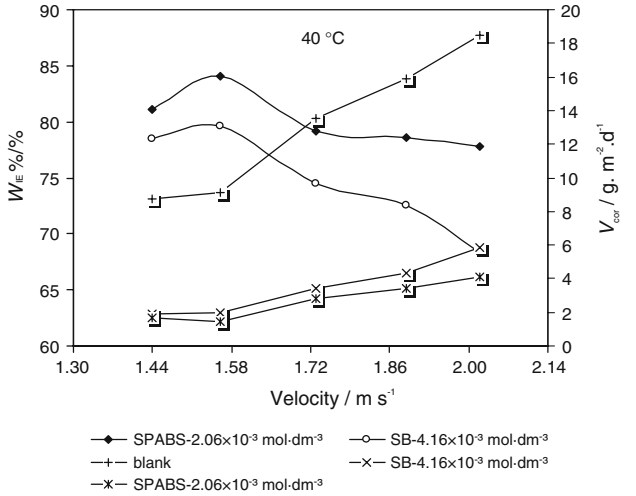

Fig. 7 Effect of fluid velocity on w_{IE} % of SB and SPABS on low carbon steel in industrial water at optimum concentrations and at 40 °C

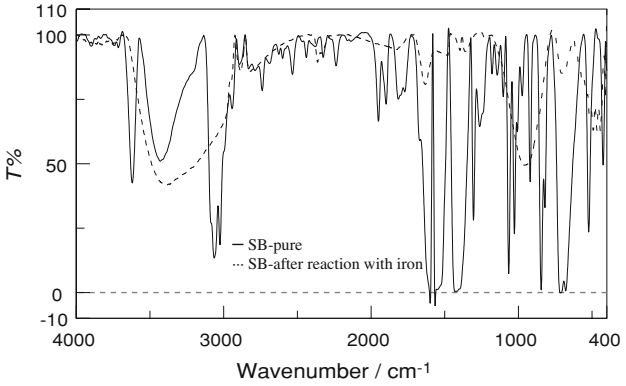

Fig. 8 FT-IR spectra of SB before and after its reaction with iron at optimum conditions

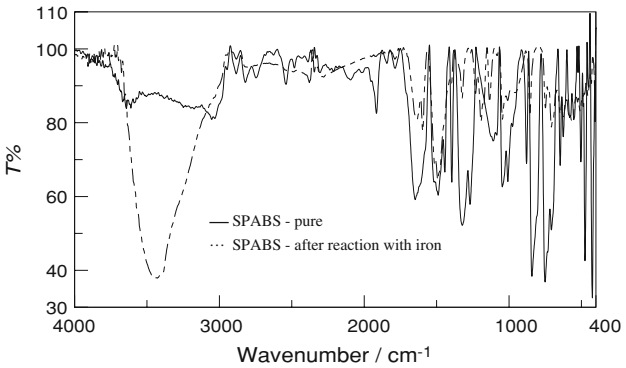

Fig. 9 FT-IR spectra of SPABS before and after its reaction with iron at optimum conditions

adsorbed film from the metal surface. Also, the mechanical effects act by breaking down the adsorbed layer, and the thinner laminar layer along the metal surface is reduced at higher velocity.

Changes in entropy, enthalpy, and activation energy of the processes are also noticed at different velocities. Experimentally, it was found that at 303 K the values of entropy are -188.7 J mol^{-1} K^{-1} at 1.56 m s^{-1} and -185.7 J mol^{-1} K^{-1} at 1.44 m s^{-1} in an uninhibited solution. Thus, 1.56 m s^{-1} is the optimal velocity for the studied inhibitors. The relatively high inhibition efficiency obtained with SPABS (Figs. 4, 7) rather than SB may be attributed to the presence of two phenyl groups which lead to stronger bonding through the overlap of the π-orbital of the phenyl ring with the metal *d*-orbital, resulting in firmer adsorption. Further, the presence of sulfur atom and amino group share the electrons with the *d*-orbital of metal.

FT-IR analysis

The FT-IR analysis of the investigated compounds before and after their reaction with iron were carried out between 400 and 4,000 cm^{-1}. The spectra are shown in Figs. 8 and 9. The peak at around 2,800–3,050 was assigned to aromatic C–H stretch. C = O and C–O stretching frequencies are shown at 1,590 and 1,414 cm^{-1}. The FT-IR spectrum of SB after reaction with iron is shown in Fig. 8. Shifting of C = O stretching frequency from 1,590 cm^{-1} to 1,620 cm^{-1} and C–O stretching mode from 1,414 cm^{-1} to 1,375 cm^{-1} indicates that COO^- may attach to the metal [25]. The broad envelope between 3,000 and 3,600 cm^{-1} is due to the presence of water in the iron complex. The N–H stretch of SPABS is shown around 3,150 cm^{-1} and N–H bending mode is observed at around 1,490 cm^{-1}. S=O and S–O stretching modes are shown at 1,220 and 1,047 cm^{-1}. The FT-IR spectrum of SPABS after reaction with iron is shown in Fig. 9. A broad envelope in the higher energy side is due to the presence of water in the complex, and shifting of SO_3^- stretching frequencies to the lower frequency side indicate the presence of SPABS over the iron surface.

Conclusion

SB and SPABS are efficient inhibitors for low carbon steel in industrial water. Optimization of temperature, inhibitor's concentration and fluid velocity have been made. At optimum concentration and fluid velocity, and at all examined temperatures, w_{IE} % reaches to 81.5 and 84.4% for SB and SPABS. The w_{IE} % of SB and SPABS were found to increase with increasing concentration leading to a decrease of apparent activation energy of the corrosion process. The adsorption of the studied inhibitors is well described by the Freundlich isotherm model. Thermodynamic parameters indicated that the adsorption of SB and

SPABS on low carbon steel surface is physisorption. The adsorbed films containing the investigated compounds were identified by FT-IR spectral analysis.

Experimental

Materials and methods

Sodium benzoate (SB) and sodium 4-(phenylamino)benzenesulfonate (SPABS) were used as received (both Merck). Figure 10 shows the chemical structures of the investigated organic compounds. Corrosion studies have been made on low carbon steel rings, cut from low carbon steel pipes 5.02 mm long, 19.18 mm outside diameter and 1 mm thick. The composition (wt %) of the low carbon steel was: 0.15 - C; 0.37 - Si; 0.04 - P; 0.01 - Al; 0.05 - Mn; 0.05 - S and the reminder iron. The pH of the industrial water used was 6.9 and the chemical composition (ppm) was: 1.19×10^5 - Cl^-; 950 - Ca^{2+}; 650 - SO_4^{2-}; 450 - Mg^{2+}; 64 - HCO_3^-. Prior to each experiment, the surface of the specimen was polished with emery paper (grade 220–600) in order to eliminate the heterogeneities caused by cutting, then washed by running tap water, washed by distilled water and dried in air, immersed in benzene (caution: due to its cancerogenity benzene should only be handled in a hood) for 5 s and dried on tissue paper, immersed in acetone for 5 s and dried on tissue paper. The specimen was annealed in an oven for half an hour to remove the mechanical stress, then cooled at room temperature and kept in a desiccator over silica gel until use. The chamber used in this test was a round flask (diameter, $D_t = 128.5$ mm) with three terminating necks containing 1 dm^3 of an electrolyte-inhibitor solution. The specimen was held on the end of the motor shaft and immersed in the chamber. The temperature of the environment was maintained by a thermostatically controlled water bath (Sonar, New Delhi, India). The velocity of the specimen was set using a speed-regulated rotating motor (Eltek, Mumbai, India). The initial mass of the specimen was recorded using an analytical balance (precision ± 0.1 mg) before immersion in the industrial water. Gravimetric results obtained are at least from three experiments to ensure reproducibility. The corrosion rates of low carbon steel have been determined for 7 h of immersion period at various rotational speeds (1,500–2,100 rpm) from mass loss using Eq. (10), where Δm is mass loss (g), t is the immersion time (d), and A is the area of the cylinder coupon (m^2). The corrosion rate (v_{cor}) is expressed in g m^{-2} day^{-1}.

$$v_{cor} = \frac{\Delta m}{t \cdot A} \tag{10}$$

The adsorbed film on the metal surface during the experiments in the presence of inhibitors were washed with distilled water, dried and scraped out from the specimen's surface and used for subsequent spectral analysis. IR spectra were recorded using a JASCO FT-IR-4100 spectrophotometer using KBr discs.

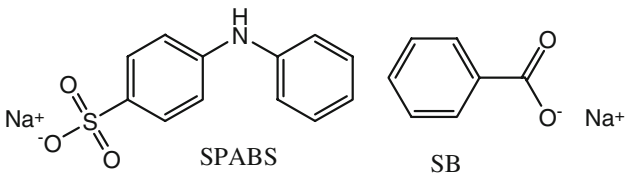

Fig. 10 Chemical structures of SB and SPABS

References

1. Bentiss F, Lagrenee M, Trainsnel M, Hornez JC (1999) Corros Sci 41:789
2. Bentiss F, Lagrenee M, Trainsnel M (2001) J Appl Electrochem 31:41
3. Qiu LG, Xie AJ, Shen YH (2005) Corros Sci 47:237
4. Divakara Shetty S, Prakash Shetty, Sudhakaer HV (2007) Mater Lett 61: 2347
5. Bentiss F, Lebrini M, Lagrenee M (2005) Corros Sci 47:2916
6. Damborenea J De, Bastidas JM, Vazquez AJ (1996) Electrochim Acta 42: 455
7. Aramaki K, Oya T, Fuji S, Gijutsu B (1961) Corros Eng 31:519
8. Bastidas JM, Damborenea J De, Vazquez AJ (1997) J Appl Electrochem 27: 345
9. Sastry VS (1998) Corrosion Inhibitors: Principles and Applications. Wiley, New York
10. Sinnott RK (1983) Chemical Engineering, vol 1, 1st edn. Pergamon Press, Oxford
11. Moretti G, Quartarone G, Tassan A, Zingales A (1994) Werkst Korros 45:641
12. Nageh Allan K (2007) Appl Surf Sci 253:4573
13. Benali O, Larabi L, Traisnel M, Gengembre L, Hraek Y (2007) Appl Surf Sci 253:6136
14. Wang HL, Fan HB, Zheng JS (2002) Mat Chem Phys 77:655
15. Durnie W, Marco RD, Jeferson A, Kinsella B (1999) J Electrochem Soc 146:1751
16. Warren L, Julian CS, Peter H (1985) Unit operations of chemical engineering, 4th edn. McGraw Hill, pp 217, 219, 690
17. Jain PC, Monika Jain (2003) Engineering chemistry, 14th edn, Dhanpat Rai, New Delhi
18. Ivanov SS (1986) Inhibitors for metal corrosion in acid media: metallurgy, Moscow
19. Mernari B, Elkadi L, Kertit S (2001) Bull Electrochem 17:115
20. Riggs OL Jr, Hurd RM (1967) Corrosion 23:252
21. Schmid GM, Huang HJ (1980) Corros Sci 20:1041
22. Bentiss F, Lebrini M, Lagrenee M (2005) Corros Sci 47:2916
23. Butler G, Stroud G (1965) J Appl Chem 15:352
24. Sinnott RK (1985) Chemical Engineering Series, vol 6, 1st edn. Pergamon, Oxford
25. Robinson SD, Uttleys MF (1973) J Chem Soc 12:1912